Established in 1871

Swiss Medical Weekly

Formerly: Schweizerische Medizinische Wochenschrift
An open access, online journal • www.smw.ch

Original article | Published 04 May 2021 | doi:10.4414/smw.2021.20487
Cite this as: Swiss Med Wkly. 2021;151:w20487

Dynamic modelling to identify mitigation strategies for the COVID-19 pandemic

Hossein Gorji[a*], Markus Arnoldini[b*], David F. Jenny[c], Wolf-Dietrich Hardt[d**], Patrick Jenny[e**]

[a] Laboratory of Multiscale Studies in Building Physics, Empa, Swiss Federal Laboratories for Materials Science and Technology, Dübendorf, Switzerland
[b] Department of Health Sciences and Technology, Swiss Federal Institute of Technology, Zurich, Switzerland
[c] Department of Mathematics, Swiss Federal Institute of Technology, Zurich, Switzerland
[d] Institute of Microbiology, D-BIOL, Swiss Federal Institute of Technology, Zurich, Switzerland
[e] Department of Mechanical and Process Engineering, Swiss Federal Institute of Technology, IFD, Zurich, Switzerland

* Equally contributing first authors; ** Equally contributing last authors

Summary

Relevant pandemic-spread scenario simulations can provide guiding principles for containment and mitigation policies. We devised a compartmental model to predict the effectiveness of different mitigation strategies with a main focus on mass testing. The model consists of a set of simple differential equations considering the population size, reported and unreported infections, reported and unreported recoveries, and the number of COVID-19-inflicted deaths.

We assumed that COVID-19 survivors are immune (e.g., mutations are not considered) and that the virus is primarily passed on by asymptomatic and pre-symptomatic individuals. Moreover, the current version of the model does not account for age-dependent differences in the death rates, but considers higher mortality rates due to temporary shortage of intensive care units. The model parameters have been chosen in a plausible range based on information found in the literature, but it is easily adaptable, i.e., these values can be replaced by updated information any time. We compared infection rates, the total number of people getting infected and the number of deaths in different scenarios. Social distancing or mass testing can contain or drastically reduce the infections and the predicted number of deaths when compared with a situation without mitigation. We found that mass testing alone and subsequent isolation of detected cases can be an effective mitigation strategy, alone and in combination with social distancing. It is of high practical relevance that a relationship between testing frequency and the effective reproduction number of the virus can be provided. However, unless one assumes that the virus can be globally defeated by reducing the number of infected persons to zero, testing must be upheld, albeit at reduced intensity, to prevent subsequent waves of infection.

The model suggests that testing strategies can be equally effective as social distancing, though at much lower economic costs. We discuss how our mathematical model may help to devise an optimal mix of mitigation strategies against the COVID-19 pandemic. Moreover, we quantify the theoretical limit of contact tracing and by how much the effect of testing is enhanced, if applied to sub-populations with increased exposure risk or prevalence.

Introduction

The recent outbreak of COVID-19 in Wuhan, China has led to a pandemic with significant impacts on public health and economies across the globe. As the number of infected people increases in a community, public health policies move away from containment of the outbreak to mitigation strategies such as social distancing and isolation, with considerable detrimental effects on public life and the economy. Although less restrictive mitigation strategies would be desirable, alternative choices are limited owing to a lack of resources and technologies. To better understand the potential effects of a particular mitigation strategy, we must assess the underlying factors that impact the spread of the

outbreak, and for this mathematical models integrating the relevant underlying mechanisms are a good tool.

Various biomathematical approaches have been proposed and pursued for epidemic-spread modelling. At the highest level, one can categorise them into agent based [1], network [2, 3] and compartmental models [4]. The chosen model can then be closed using empirical/machine-learning, statistical or deterministic approaches [5]. Agent/network based models may provide highly refined scenario analysis tools, but their black-box nature may not be appropriate for large-scale mitigation scenario assessments. Compartmental models, on the other hand, can provide us with insightful and explicit solutions more relevant for drawing fundamental conclusions. These type of models may employ deterministic or stochastic methodologies to tackle the evolution of the epidemic within a susceptible population. The former category belongs to deterministic descriptions, which include susceptible-infectious-removed (SIR), susceptible-infectious-susceptible (SIS) and susceptible-exposed-infectious-removed (SEIR) models [6]. A more complicated class of models incorporates the stochastic nature of the epidemic spread via the framework of, for example, Ito- or Levy-type processes [7–9]. Both deterministic and stochastic descriptions, at their fundamental level, rely on reaction mechanisms that characterise infections, recoveries and deaths within different subgroups of the population.

Although recently there has been a massive effort in pandemic-spread investigations of COVID-19, for example using SEIR models [10–13], network models [14] and agent-based simulations [15, 16], no studies that investigated the effect of mass testing are found in the literature. As recent efforts in, for example, China are channelled towards mass testing in relatively large cities [17], it is necessary to also provide theoretical foundations for mass testing-based mitigation strategies. To achieve this, we separated the category of detected cases from infected ones who remain undetected (e.g., by the sheer lack of test kits) and predicted their coupled dynamics. Note that detected here refers to persons being isolated, which comprises not only those who tested positive, but also those who have strong symptoms and thus stay in self-quarantine. It is also important to note that in the case of this specific virus, the asymptomatic and pre-symptomatic infected people contribute significantly to the spread of the pandemic [18]. Therefore, early detection and containment of infected but asymptomatic individuals can be extremely relevant for the dynamic behaviour. Hence, we devised a set of reaction equations focusing on both detected and undetected categories. Moreover, the impact of the shortage of intensive care units during peaks of the pandemic were integrated in the outcome of the scenarios. The model coefficients were calibrated on the basis of existing data, and the model was employed to investigate two main mitigation approaches, one relying on social distancing and one on more frequent infection testing. Also, a combination of the two is studied, and we quantified by how much the testing efficiency is enhanced, if available resources are focused on subpopulations with increased prevalence. Finally, theoretical limitations of contact tracing, which relies on isolating contacts of symptomatic individuals, was studied. We argue that as contact tracing provides little means to prevent virus transmission from asymptomatic cases, it cannot lead to the pandemic containment as a stand-alone approach.

Materials and methods

A model was proposed to compute the numbers of infected people whose infection had not (yet) been detected and the numbers of infected persons with a detected infection (n_i^{undet} and n_i^{det}), respectively (fig. 1).

Note that detected here refers to persons being isolated, which comprises not only those who tested positive, but also those who have strong symptoms and thus stay in self-quarantine. It is further important to notice that in the case of SARS-CoV2, the undetected infected people are main contributors to the spread of the pandemic [18]. The exact definitions of detected and undetected, as well as those of all other variables and model parameters are found in table 1.

Furthermore, we computed the number of fatalities (n_d) and the number of people who recovered after a detected or an undetected infection. Importantly, we assumed that these people would have developed protective immunity and we assumed that they cannot be infected again in the time frame considered. The initial susceptible population n_s^0 is naive (i.e., it lacks immunity against the infection) and n_s is the number of persons who are susceptible at a given time t. In our model we assumed that the virus is mainly passed on by undetected asymptomatic and mildly symptomatic persons; the detected population with mild symptoms transmits at a much lower rate (because of self-isolation, hygiene precautions in hospitals and/or quarantine). Although our model does not explicitly consider age specific mortality, we did take into account that 40% of the hospitalised cases need intensive care, and that at the peak, the case fatality ratio increases two-fold because of pressure in healthcare systems. The graph in figure 1 shows the dynamic dependencies. The COVID-19-specific parameters had to be estimated from the available data; their values are listed below. It should be noted that the implementation of our model allows our current estimates to be updated with more precise values, as new data come in.

Table 1: Terminology and nomenclature of model parameters and variables.	
Terminology	**Meaning**
Susceptible	Persons of the considered population who are susceptible and thus can potentially get infected
Exposed	Infected persons; cannot yet transmit the virus
Asymptomatic	Infected persons without symptoms; can transmit the virus
Pre- and mild sympt. (no self isol.)	Infected persons with no or mild symptoms; infectious, but not isolated
Mild sympt. (self isol.)	Infected persons with mild symptoms; infectious and isolated
Strong symptomatic	Infected persons with strong symptoms and thus hospitalised; isolated
Deceased	Persons who died
Recovered	Persons who recovered
Detected	Isolated either after positive testing or after falling ill
Undetected	Persons who are either exposed, asymptomatic or mildly symptomatic, but were never contained
Extreme social distancing	$\mathcal{R}_{\text{eff}} = 0.7$, if no other mitigation measures are applied; the infection rate is reduced by 71%
Moderate social distancing	$\mathcal{R}_{\text{eff}} = 1.0$, if no other mitigation measures are applied; the infection rate is reduced by 58%
Mild social distancing	$\mathcal{R}_{\text{eff}} = 1.6$, if no other mitigation measures are applied; the infection rate is reduced by 33%
Variable	
n_s and n_s^0	Numbers of susceptible and initially susceptible persons, respectively
n_e, $\widetilde{n}_e$ and n_e^{tot}	Numbers of exposed persons; not tested, tested and in total, respectively
n_{ia}, $\widetilde{n}_{ia}$ and n_{ia}^{tot}	Numbers of asymptomatic persons; not tested, tested and in total, respectively
n_{im}, $\widetilde{n}_{im}$ and n_{im}^{tot}	Numbers of persons with mild symptoms during first day; not tested, tested and in total, respectively
n_{ms}, $\widetilde{n}_{ms}$ and n_{ms}^{tot}	Numbers of persons with mild symptoms after first day; not tested, tested and in total, respectively
n_{ss}, $\widetilde{n}_{ss}$ and n_{ss}^{tot}	Numbers of persons with strong symptoms; not tested, tested and in total, respectively
n_d, $\widetilde{n}_d$ and n_d^{tot}	Numbers of deceased persons; not tested, tested and in total, respectively
n_{ra}, $\widetilde{n}_{ra}$ and n_{ra}^{tot}	Numbers of recovered persons who had no symptoms; not tested, tested and in total, respectively
n_{rs}, $\widetilde{n}_{rs}$ and n_{rs}^{tot}	Numbers of recovered persons who had symptoms; not tested, tested and in total, respectively
n_i^{undet}	Undetected infected persons: $n_{ie} + n_{ia} + n_{im}$
n_i^{det}	Detected infected persons: $n_{ms} + n_{ss} + \widetilde{n}_{ms} + \widetilde{n}_{ss} + \widetilde{n}_{ie} + \widetilde{n}_{ia} + \widetilde{n}_{im}$
Parameter	
β and $\widetilde{\beta}(\tau)$	Rate coefficient for infection and expected infectiousness τ days after infection, respectively
Q	Relative infection rate by outside contact (travel)
ϵ	Ratio between infection rate of self-quarantined and non-quarantined symptomatic cases
α_a and α_s	Rate coefficient for latency of asymptomatic and symptomatic cases, respectively
θ	Rate coefficient for mortality of hospitalised cases
γ_a, γ_{ms} and γ_{ss}	Rate coefficients for recovery
ξ_{ms} and ξ_{ss}	Rate coefficients for successively stronger symptoms
k_e, k_a and k_s	Rate coefficients accounting for testing
$\mathcal{R}_0$	Basic reproduction number without mitigation
$\mathcal{R}_{\text{eff}}$	Effective reproduction number with mitigation
$\mathcal{R}_{\text{eff}}^{symp}$ and $\mathcal{R}_{\text{eff}}^{asym}$	Effective reproduction number of symptomatic and asymptomatic cases, respectively
$\mathcal{R}_{\text{eff}}^{wt}$	Effective reproduction numbers subject to testing, respectively
κ	Fraction of basic reproduction number related to symptomatic cases
ζ	Percentage of app users among smart-phone owners
$\theta^{(sat)}$ and $\theta^{(0)}$	Rate coefficient for mortality of hospitalized cases without and with intensive care units, respectively
$\gamma_{ss}^{(sat)}$ and $\gamma_{ss}^{(0)}$	Rate coefficient for recovery of hospitalized cases without and with intensive care units, respectively
N	Testing interval
N^{-1}	Testing frequency
η	Fraction of false negative test results
$C^{(sat)}/2.5$	Fraction of total population for which intensive care units are available
Operator and function	
$\mathbb{E}(\cdot)$	Expectation
$\mathcal{P}_{\mathcal{A}}$ and $\text{Prob}\{\mathcal{A}\}$	Probability of the event $\mathcal{A}$

Figure 1: Graphical representation of the model. The graph showing the dependencies of the compartments describing the transmission dynamics among susceptible people.

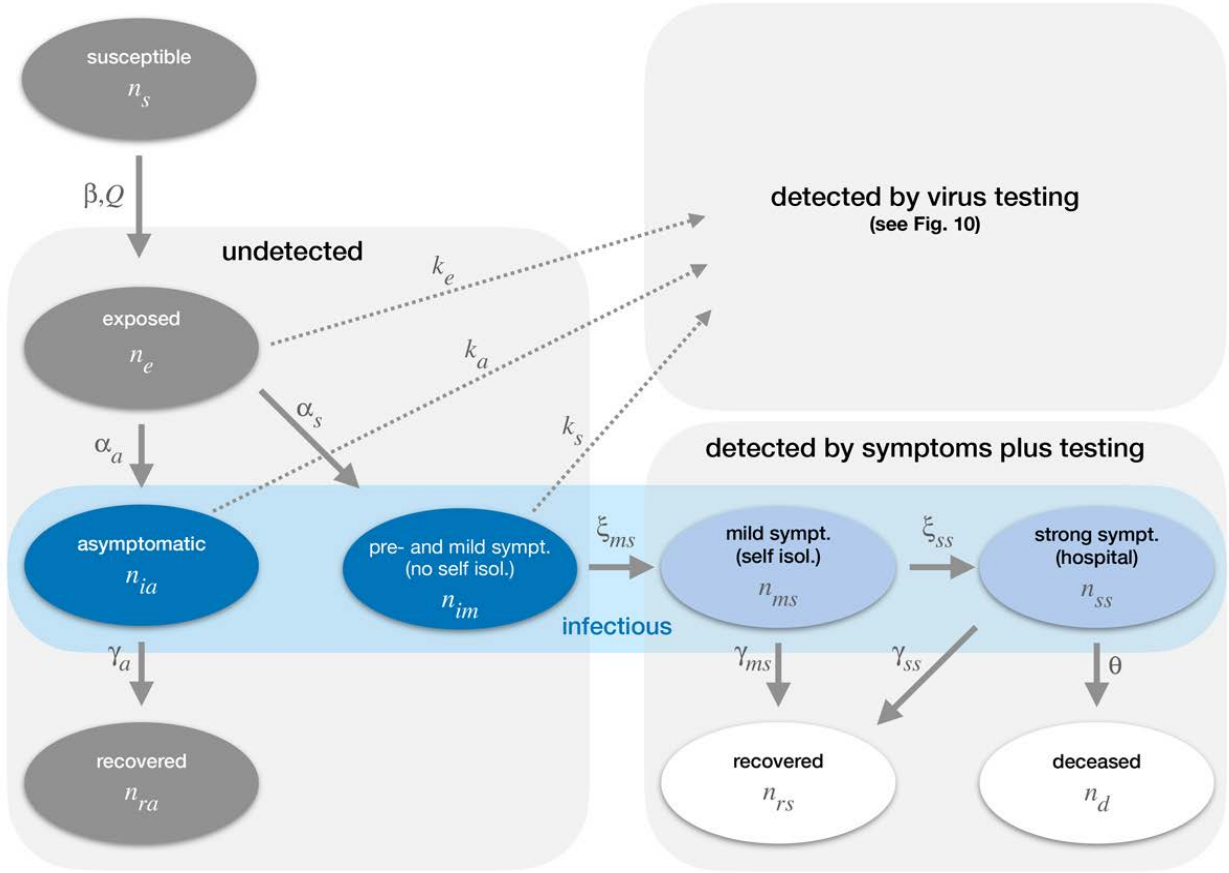

Initially, the entire population is susceptible and can get infected. Infected persons first get exposed and are not infectious until the latency time has passed. Then they are either asymptomatic or mildly symptomatic. Asymptomatic persons eventually recover without symptoms, whereas the others develop symptoms approximately half a day after the end of the latency period. We assumed that persons with mild symptoms isolate themselves approximately 1 day after onset of symptoms and then either recover or become strong symptomatic, which requires hospitalisation. Hospitalised individuals either recover or die. Once n_s becomes smaller, which happens quickly without any measures, the susceptible contact rate slows down by a factor of n_s/n_s^0. This mechanism of slowing spread of the epidemic owing to a shrinking susceptible population is equivalent to herd immunity. It is crucial for the system dynamics that detected persons are isolated (either by self-isolation at home, by hygienic isolation in a hospital setting or in other care facilities, or by organised isolation programmes for detected infected people, such as in hotel rooms) and thus participate at a much lower rate or not at all in spreading the disease. We assumed that these detected infected people have a 10-fold lower likelihood of infecting others than undetected infected people. All this leads to a dynamic system, which is governed by a set of ordinary differential equations (equations (10)–(26)). The effect of testing is further discussed in the section on "Mass testing" below. Next we describe how the parameters can be estimated based on literature data.

Parameter estimation

Our generalised SEIR model became closed once we tuned the rate coefficients. These coefficients were mainly computed based on data provided in recently published reports [12, 19]. Before giving the values for transfer rates between different compartments, let us analyse the basic reproduction number $\mathcal{R}_0$ of this virus infection with $Q = 0$ and $n_s(t) \approx n_s^0$. Note that $\mathcal{R}_0$ represents "the expected number of secondary cases produced, in a completely susceptible population, by a typical infective individual" [20]. If $\mathcal{R}_0$ becomes < 1, virus spread will decline, and if $\mathcal{R}_0 > 1$, virus spread will increase. Derivation of $\mathcal{R}_0$ based on the next generation method is explained in the section on "Basic and effective reproduction numbers" in the appendix. By inspecting equation (28), we observe that the disease-free equilibrium (DFE) corresponding to $\mathcal{R}_0 \leq 1$ can be achieved by reducing the infection rate β via mitigation

policies such social distancing. Importantly, as shown later, $\mathcal{R}_0$ can be reduced as well by introducing mass testing, contact tracing, targeted testing and subsequent isolation of detected infected individuals.

Next, to clarify our choice of model coefficients, we discuss the rates which appear in infectious and non-infectious compartments separately. Finally, the increase of mortality due to lack of intensive care units was modelled.

Infectious

We modelled the incubation time to be log-normally distributed with mean 5.84 days and standard deviation 2.98 days [21, 22]. In accordance with [19], we took the latency time x_l such that on average it becomes half a day shorter than the incubation time. As for the incubation time, we adopted a log-normal distribution for x_l but with mean 5.34 days and standard deviation 2.7249 days. We assumed that $1/3$ of the cases would not have noticeable symptoms and $2/3$ become symptomatic half a day after latency [19]. This led to $\alpha_a = \frac{1}{3}\mathbb{E}(1/x_l) = 0.078$ (1/day), where $\mathbb{E}(\cdot)$ denotes the expectation which gave us the average latency rate. Because of the ratio of $1/3$ to $2/3$ between asymptomatic and symptomatic cases we got the transfer rate from being exposed to infectious symptomatic as $\alpha_s = 2\alpha_a = 0.156$ (1/day).

We supposed that it takes around 1 day from onset of symptoms to self-isolation [19]. Since it takes half a day time delay from becoming infectious to symptomatic, we got $\xi_{ms} = 1/1.5 = 0.6667$ (1/day).

The average onset to discharge time of clinical cases is around 22 days [23]. We assumed that for mildly symptomatic cases the onset to recovery time would be half of this time, i.e., around 11 days. Therefore the average recovery time from end of the latency period becomes 11.5 days for mild-symptomatic cases. We set the same recovery time for asymptomatic cases which led to $\gamma_a = 1/11.5 = 0.087$ (1/day).

A range of values have been suggested for infectiousness of asymptomatic cases: 0.1 in [24], 2/3 in [19] and 1 in [23]. We assumed that the asymptomatic cases were 50% less infectious. Furthermore we considered the self-quarantined patients to be 90% less infectious, i.e., $\epsilon = 0.1$ was adopted. To compute the infection rate β, we assumed $\mathcal{R}_0 = 2.4$ [24, 25]. Following equation (28), the infection rate becomes $\beta = 0.6711$ (1/day). Since the basic reproduction number is the most important single parameter of the system, we performed sensitivity studies by changing $\mathcal{R}_0$ [26].

Non-infectious

The mean delay time from appearance of symptoms to hospitalisation has been reported to be around 11 days [23]. However, 80% of symptomatic cases would not require hospitalisation [27]. For those who develop strong symptoms, the delay from self-isolation to hospitalisation then becomes $11 - 1 = 10$ days. Hence we got $\xi_{ss} = 0.2 \times 1/10 = 0.02$ (1/day) and $\gamma_{ms} = 0.8 \times 1/10 = 0.08$ (1/day). Note that the latter gives onset to recovery time of 11 days for mild cases, which is consistent with our earlier assumption.

The average hospital treatment time is 11 days [19, 23]. In the case of availability of intensive care units, we assumed that 20% of hospitalised cases die [27, 28]. Accordingly, we got $\gamma_{ss}^{(0)} = 0.8 \times 1/11 = 0.0727$ (1/day) and $\theta^{(0)} = 0.2 \times 1/11 = 0.0182$ (1/day).

Fatality increase

We assumed that the case fatality ratio increases two-fold when there is saturation of the health system. This is justified by noting that the case fatality ratio has increased from approximately 5% in China [29] to roughly 10% in Wuhan while it was the epicentre of the outbreak [30]. By taking this factor into account, and assuming that the average time of hospital treatment remains 11 days, we could compute the death rate of hospitalised cases once saturation of intensive care units is reached as $\theta^{(sat)} = 0.4 \times 1/11 = 0.0364$ (1/day). Note that one consistently obtains $\gamma_{ss}^{(sat)} = 0.6 \times 1/11 = 0.0546$ (1/day). It was assumed that there are eight intensive care beds per 100,000 persons (UK average [19],) and that 40% of the hospitalised cases need such treatment. Note that the number of available intensive care beds varies by country. For example, in Switzerland the number is roughly estimated to be 15–17.5 beds per 100,000; in other countries this may be much lower. Accordingly, saturation is reached once the number of hospitalised cases, i.e., n_{ss}, exceeds $C^{(\mathrm{sat})} = 0.02\%$ of the total population.

The adjusted rate

$$\theta(n_{ss}^{tot}) \quad = \quad \frac{n_s^0}{n_{ss}^{tot}}\left(\min\left\{C^{(\mathrm{sat})}, \frac{n_{ss}^{tot}}{n_s^0}\right\}\theta^{(0)} + \max\left\{0, \frac{n_{ss}^{tot}}{n_s^0} - C^{(\mathrm{sat})}\right\}\theta^{(\mathrm{sat})}\right) \tag{1}$$

then quantifies the death rate of hospitalised cases as the weighted average of $\theta^{(0)}$ and $\theta^{(\mathrm{sat})}$; the consistently adjusted recovery rate became

$$\gamma_{ss}(n_{ss}^{tot}) \quad = \quad \gamma_{ss}^{(0)} + \theta^{(0)} - \theta(n_{ss}^{tot}). \tag{2}$$

All estimates here are summarised in table 2; note that these values can easily be adapted, if more reliable data become available.

Table 2: Estimates made for the model closure, social distancing, contact tracing and testing.

Probability	**Conditional on**	**Expression**	**Base case value**
Pre- and mild sympt. (no self isol.)	Asympt.	$S^{(m)}$	2/3, [1/2, 2/3]
Strong sympt. (hospit.)	Mild sympt. (self isol.)	$S^{(s)}$	1/5
Deceased	Hospit.; with icu	$M^{(0)}$	1/5
Deceased	Hospit.; no icu	$M^{(sat)}$	2/5
Char. time scale (days)			
Pre- and mild sympt. (no self isol.)	Exposed	$S^{(m)}\alpha_s^{-1}$	4.27
Mild sympt. (self isol.)	Pre- and mild sympt. (no self isol.)	$t_{im} = \xi_{ms}^{-1}$	1.5
Strong sympt. (hospit.)	Mild sympt. (self isol.)	$t_{ms} = S^{(s)}\xi_{ss}^{-1}$	10
Deceased	Str. sympt.	$M^{(0,sat)}/\theta^{(0,sat)}$	11
Recovered	Asymptomatic	$t_{ia} = \gamma_a^{-1}$	11.5
Further parameters			
Basic reproduction number		$\mathcal{R}_0$	2.4
Infection rate reduction factor	Mild sympt. (self isol.)	ϵ	0.1
Rel. intensive care capacity		$C^{(sat)}/2.5$	0.00008
Social distancing, contact tracing and testing			
Infection rate reduction factor	Social distancing	λ	0
Testing frequency (1/days)	Testing	N^{-1}	0
Testing process time (days)	Testing	τ_{proc}	1
Fraction of false negative test results	Testing	η	0.05, {0.5, 0.15, 0.25}
Success rate of contact tracing	Contact tracing	ζ	[0.3, 1]
Fraction of exposed people who develop no symptoms	Contact tracing	r_1	[1/3, 1/2]
Fraction of exposed people who develop no symptoms	Contact tracing	r_2	[0.1, 0.5]

The resulting parameter values for our base case are provided in table 3.

Table 3: List of estimated parameters and initial values.

Parameter	**Value**
β	0.670 (1/day)
ϵ	0.1
α_a	0.078 (1/day)
α_s	0.156 (1/day)
γ_a	0.087 (1/day)
ξ_{ms}	0.667 (1/day)
γ_{ms}	0.08 (1/day)
ξ_{ss}	0.02 (1/day)
$\gamma_{ss}^{(0)}$	0.072 (1/day)
$\theta^{(0)}$	0.0182(1/day)
$\theta^{(sat)}$	0.0364 (1/day)
Initial condition	**Value**
n_s^0	6,384,631,490 (world population outside of China)
$n_e(0)$	1000

Note that our model allows any of these parameters to be easily replaced by more precise estimates, as more data become available. The initial values of all numbers except n_e are set to zero.

Mass testing

We analysed how many tests are needed to bring the effective reproduction number $\mathcal{R}_{\text{eff}}$ below 1 in the absence of other interventions. In practice, Slovakia, Vienna and the Swiss Canton Graubünden have recently assessed mass testing as a mitigation strategy. This showed that this is in principle possible and that the motivation to participate is quite important. In contrast to the approach described by us here, the former two campaigns have not employed repetitive testing of the population over longer periods of time. Therefore, the logistic challenges, upholding the motivation of the participants and the effectiveness in a real-life setting remain to be tested. Nonetheless, the parameters of our model could be adjusted to account for the observed effects. Thereby, the tool could provide an even more realistic prediction of the expected effects. If repetitive testing can be maintained at the same rate until a major fraction of the population is vaccinated, a new outbreak of the pandemic (i.e., a sudden exponential rise in the incidence) can be avoided. Therefore, we studied how $\mathcal{R}_{\text{eff}}$ varied once confirmed cases are isolated (in addition to self-quarantined and hospitalised individuals). Of particular value is the relationship between $\mathcal{R}_{\text{eff}}$ and the interval between tests

in the susceptible population (i.e., the frequency of testing needed for reducing $\mathcal{R}_{\text{eff}}$ below 1). Thereby we can determine the key technical parameter of interest, i.e., the number of tests per 100,000 people who must be tested per day in order to achieve the desired $\mathcal{R}_{\text{eff}}$ value; we chose $\mathcal{R}_{\text{eff}} = 1$ as the target value for our analyses (if not indicated otherwise), which would suffice to keep the number of infected people constant.

To be realistic, we supposed that the processing time τ_{proc} of mass testing would be somewhere between half a day and two days. Furthermore, a fraction $\eta = 0.05$ of false negative test results was taken into account [31]. It should be noted, however, that this is a rough estimate. The use of standards allows for very high reproducibility of virus RNA detection even between different laboratories [32]. The true rate of false negatives and false positives is currently not known. We assumed that a false negative rate of 5% is a conservative estimate. The current virus RNA testing capacities in continental Europe are up to 300 tests per 100,000 people per day (e.g., in Switzerland 2020/21). If equipment and supplies are not limiting for testing, such as by using a quantitative polymerase chain reaction (qPCR) method, we estimated that up to around 1000 samples per machine can be analysed within a time frame of 8 hours. Mass testing (i.e., if $> 500 - 1{,}000$ tests per 100,000 people per day would be required) could be realisable by taking advantage of next-generation RNA extraction, reverse transcription and sequencing (combined with reverse transcription and PCR) to detect virus RNA in infected people. For example, in [33] a massively parallel diagnostic assay is described for testing up to 19,200 patient samples per work flow. In principle, such very high-throughput approaches can be parallelised (and potentially optimised) to provide millions of tests per day. In reality, the logistics of collecting these millions of samples would be a major hurdle. Nevertheless, estimating these numbers in a quantitative fashion is instructive and might help to modify the mitigation strategy. First, we wanted to assess how many tests were necessary to stop the virus spread (i.e., to reach $\mathcal{R}_{\text{eff}} \leq 1$ if no other mitigation strategies were applied).

Obviously, the hypothetical scenario that the whole susceptible population is screened by a test with perfect sensitivity at once, would lead to the trivial disease-free state. However, this is an unrealistic scenario, not only because of a lack of test capacity, but also due to logistic and compliance concerns, and false negative test results. Therefore, it is only realistic to assume that individuals would be tested according to different schedules. Let us consider a situation where each person is tested once every N days. Note that this is equivalent to testing a random fraction of $1/N$ of the susceptible population every day. Therefore we focussed on the set $\{1, \ldots, N\}$ of days. An individual is infected at some random time x. To characterise x, we assumed that the likelihood of getting infected does not vary much during these days, which is justified if testing is applied at an intensity such that $\mathcal{R}_{\text{eff}} \approx 1$. Hence x becomes uniformly distributed in the interval $[1, N]$. The time delay between infection and detection would then be $\tau_{det} = N - x + \tau_{proc}$. Finally, we sampled the latency time x_l from a log-normal distribution with 5.34 ± 2.7249 (see the section on "Parameter estimation" above).

Intuitively, by conducting mass testing on individuals who are neither self-quarantined nor hospitalised, positive cases will be detected from exposed, asymptomatic and mild-symptomatic compartments. To quantify each detection rate, it is essential to compare detection time versus the latency period; therefore we consider the effect of testing on these three compartments individually:

Exposed

When an infected individual is tested during the latency period, they would be detected from the exposed compartment. This translates into an event set $\mathcal{A}: \tau_{det} \leq x_l$. The rate of detecting individuals by testing from the exposed population is then

$$k_e \quad = \quad (1-\eta)\mathcal{P}_{\mathcal{A}}\mathbb{E}_{\mathcal{A}}[\tau_{det}^{-1}] \qquad (3)$$

where $P_{\mathcal{A}}$ and $\mathbb{E}_{\mathcal{A}}$ denote frequency of such events and conditional expectation, respectively.

Mildly symptomatic

When testing is after the latency period, there are two types of infection development. According to our setting, two thirds of the infected individuals would develop symptoms that would lead them to self-isolate. Please note, that the fraction of infected individuals who remain asymptomatic may range between 33% and 50% [19, 24, 34]; see table 2. Therefore, we also tested scenarios where 60% or 50% of infected develop symptoms; see fig. 9 below. These individuals may turn to testing centres in order to detect the virus and incentivise the decision for self-quarantine. They can be detected by testing and therefore sent into quarantine within 1½ days after becoming infectious. The relevant event set is $\mathcal{B}: (\tau_{det} \geq x_l) \cap (\tau_{det} \leq (x_l + 3/2))$, from which one obtains

$$k_s \quad = \quad \tfrac{2}{3}(1-\eta)\mathcal{P}_{\mathcal{B}}\mathbb{E}_{\mathcal{B}}[\tau_{det}^{-1}] \qquad (4)$$

for the test detection rate of mild-symptomatic persons.

Asymptomatic

This is arguably the most important group to consider, because they will not know that they are infected and they can make up as much as 50% of the entire group of the infected people. Importantly, they are very hard to identify

using the current mitigation strategies, including app-based contact tracing [24]. We discuss this in more detail, below. Testing may catch asymptomatic cases. These individuals will not have symptoms and would recover after 11.5 days. In the first 1½ days they share the same time-line as mildly symptomatic cases. Therefore, in this scenario two event sets $\mathcal{B}$: $(\tau_{det} \geq x_l) \cap (\tau_{det} \leq (x_l + 3/2))$ and $\mathcal{C}$: $((\tau_{det} \geq (x_l + 3/2)) \cap (\tau_{det} \leq (x_l + 11.5))$ become relevant. We obtained the detection rate from the asymptomatic compartment from

$$k_a = \frac{1}{3}(1-\eta)\mathcal{P}_{\mathcal{B}}\mathbb{E}_{\mathcal{B}}[\tau_{det}^{-1}] + (1-\eta)\mathcal{P}_{\mathcal{C}}\mathbb{E}_{\mathcal{C}}[\tau_{det}^{-1}]. \quad (5)$$

To construct a map from testing frequency N^{-1} to $\mathcal{R}_{eff}$, we needed to find out how $\mathcal{R}_{eff}$ varies with respect to the test detection rates k_e, k_a and k_s. Hence, we defined $\mathcal{R}_{eff}^{wt}$ as the reproduction number subject to testing. In the section on "Basic and effective reproduction numbers" in the appendix, the effective reproduction number is computed for scenarios involving repetitive mass testing. It is important to emphasise that, in contrast to social distancing, the effect of testing on the reproduction number is not through reducing the infection rate (i.e., f remains the same), but rather through transfer of infected individuals to quarantine, either at home or in hotel rooms, or in care units with strict hygiene barriers, all of which would reduce the likelihood of transmission (i.e., changing V to $\widetilde{V}$).

Enhanced testing

To achieve the discussed detection rates $k_{e,a,s}$ and corresponding reductions in $\mathcal{R}_0$, the entire undetected population has to be tested once every N days (or equivalently every day a random fraction of $1/N$). To improve efficiency of testing, i.e., the probability per test of getting a positive result, the sample population can be reduced by the following approaches.

Serological testing

With serological testing, we can remove the recovered population from the pool of undetected individuals, and thus the same number of positive test results can be achieved with fewer tests. However, during an early stage of the pandemic the relative size of the undetected recovered compared with the whole undetected population is very small, and therefore the gain would be negligible. Nevertheless, this approach can easily be integrated into any mass testing strategy, for example by serological tests 1 day before the PCR tests in order to exclude immune individuals. Over time, the numbers of people with previously detected antibody titres will increase. This will reduce the number of virus RNA tests required.

Testing high prevalence sub-populations

A more effective approach would be based on an inference model (e.g., by using information from contact tracing), which allows the sample population $\mathcal{D}$ to be divided into one group $\widetilde{\mathcal{D}}$ with a higher percentage of infected individuals and the remainder. For the following analysis we denoted the size of $\mathcal{D}$ with n and that of $\widetilde{\mathcal{D}}$ with $\tilde{n}$. Further, $\tilde{p}$ is the fraction of infected persons in $\widetilde{\mathcal{D}}$ and p that in $\mathcal{D}$. Testing every person in $\widetilde{\mathcal{D}}$ at a frequency of $1/N$ would require $\tilde{n}/N$ tests per day, as opposed to n/N tests, if the whole sample population was tested. The numbers of positive test results per day, on the other hand, would be $\widetilde{P}(N) = \tilde{p}\,\tilde{n}/N$ and $P(N) = pn/N$, respectively. In order to obtain the same number of positive results from the group $\widetilde{\mathcal{D}}$ as from $\mathcal{D}$, the test interval N to $\widetilde{N}$ has to be reduced, such that $\widetilde{P}(\widetilde{N}) = P(N)$. This gives $\widetilde{N} = N(\tilde{p}\,\tilde{n})/(pn)$ and one can conclude that the number of tests required to achieve the same overall quota is reduced by the factor

$$r = \frac{\tilde{n}/\widetilde{N}}{n/N} = \frac{N\tilde{n}}{\widetilde{N}n} = \frac{p}{\tilde{p}}. \quad (6)$$

In order for this result to be practically meaningful $\widetilde{N} \geq 1$, which translates into the requirement that

$$\frac{\tilde{n}}{n} \geq \frac{r}{N}. \quad (7)$$

In short, if one can identify a group $\widetilde{\mathcal{D}} \subset \mathcal{D}$ larger than nr/N for which the percentage of infections is higher than in $\mathcal{D}$ by a factor of r^{-1}, then the number of tests needed to obtain the same reproduction number reduces by the factor r.

Results

Figure 2 shows the model results for a period of 1 year (without mitigation strategies) with $\mathcal{R}_0 \in \{1.9, 2.4, 2.9\}$ (respective plots from left to right). Dashed lines represent the immune $(n_s^0 - n_s)$, dash-dotted lines the infected $(n_i^{undet} + n_i^{det})$ and solid lines the deceased (n_d^{tot}) population.

For bigger basic reproduction numbers, one can observe a larger immune population in the endemic state (right half of the graphs), and a higher and sharper peak in the number of infections. For the remaining studies we took $\mathcal{R}_0 = 2.4$ as the base case.

The left and right plots in figure 3 show base case predictions with and without limitations in intensive care units. In both cases, 87% of the endemic population is immune, which compares well with 81% infected people predicted by [19] for the UK and US populations in the absence of mitigation plans. Without intensive care, the chance of dying for strong symptomatic people is roughly two-fold

higher than that with proper treatment (4.6 vs 2.3%). It is important to emphasise that in most European countries saturation of intensive care units did not occur owing to lockdown enforcement and other measures, especially not during the second wave. Although these numbers are subject to errors (mainly due to uncertainties in the parameter values and efforts to increase intensive care and respirator availability), it can be expected that the relevant dynamics are captured to a high degree. If the results are compared with the base case, much insight can be gained, for example into how social distancing and mass testing can be combined most effectively.

Mass testing

Using Monte-Carlo to estimate the test detection rates given by equations (3) and (4), one can compute the ratio $\mathcal{R}_{\text{eff}}^{wt}/\mathcal{R}_0$ with respect to the testing frequency N^{-1}. The plots in figures 4a and 4b show the number of tests required to reach $\mathcal{R}_{\text{eff}} = 1$. This depends on the time from sampling to result (note: we assumed immediate notification and immediate implementation of quarantine measures upon notification) and on the false negative rate (5% in fig. 4a and 15% in fig. 4b). The horizontal green dashed lines indicate $\mathcal{R}_{\text{eff}}^{wt} = 1$, if the virus reproduction rate without any mitigation is $\mathcal{R}_0 = 2.4$.

Figure 2: Predictions for a period of 1 year. with $\mathcal{R}_0 = 1.9$ (a), $\mathcal{R}_0 = 2.4$ (b) and $\mathcal{R}_0 = 2.9$ (c). Dashed lines represent the immune ($n_s^0 - n_s$), dash-dotted lines the infected ($n_i^{undet} + n_i^{det}$) and solid lines the deceased (n_d^{tot}) population. The values are in % of the initial population size and are plotted over number of days.

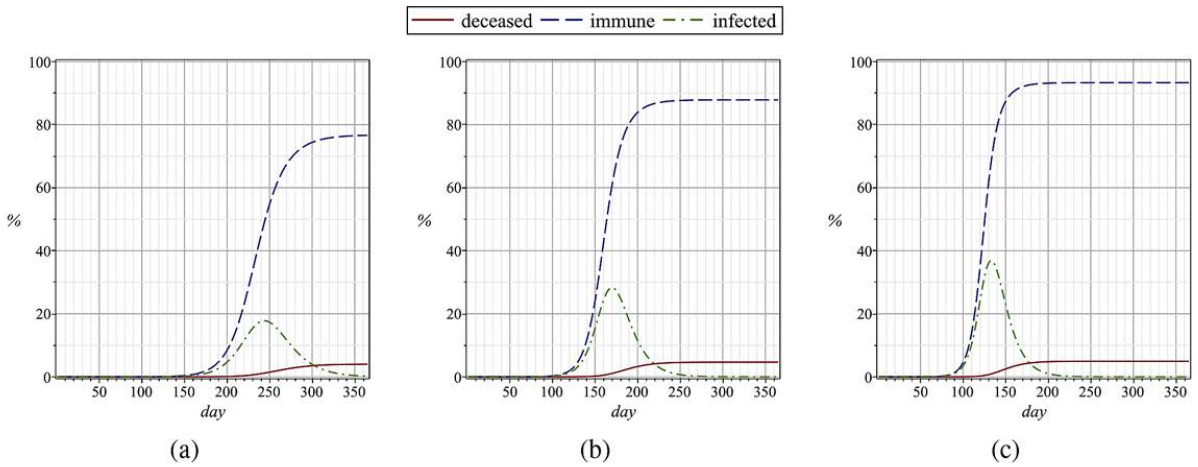

Figure 3: Base case model predictions (with $\mathcal{R}_0 = 2.4$) for a period of 1 year; left with intensive care unit limitation and right without. Dashed lines represent the immune ($n_s^0 - n_s$), dash-dotted lines the infected ($n_i^{undet} + n_i^{det}$) and solid lines the deceased (n_d^{tot}) population. The values are in % of the initial population size and are plotted over number of days.

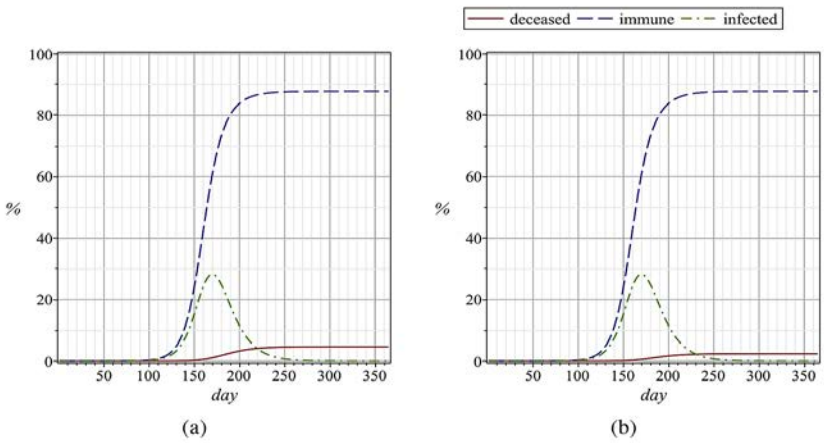

Reducing the initial $\mathcal{R}_0 = 2.4$ to 1 would the entire susceptible population to be tested roughly once every 8 days, if the false negative rate is 5%, if testing results are available after 1 day and quarantine of the detected individuals commences immediately. For half a day delay, the testing interval can be increased to roughly 12 days and for a delay of 1½ days it would be 5 days. This information is important for optimising technical development decisions. The overall testing capacity needs to be larger if the testing method requires more time (fig. 4) or if there are delays in case notification or implementation of quarantine measures. This could be justified if a low-cost technique (such as next generation sequencing, pool-testing or sufficiently sensitive antigen tests) could be devised [33].

To gain further insight into robustness and effectivity of repetitive mass testing, we set our core model parameters for the base scenario to a 1 day delay time and a 5% false negative rate. The mass testing results are shown in figure 5, subject to variations of the ratio of asymptomatic to symptomatic cases, infectiousness of asymptomatic cases, their recovery time and efficacy of isolation. Two observations can be made here.

First, as the contribution of the asymptomatic cases becomes more significant in the composition of $\mathcal{R}_0$, mass testing becomes more effective. This is due to the fact that the pre-symptomatic cases spend a much shorter time undetected in comparison with the asymptomatic ones. Therefore, in order to reduce their transmission in that short period of time, the testing frequency has to be significantly enhanced. On the other hand, once asymptomatic cases make a larger contribution in the virus transmission chain, mass testing has a longer time span to detect the virus carriers. In other words, for a fixed $\mathcal{R}_0$, if we stretch the infectiousness period of an infected case, there will be a higher chance that this case would be detected by mass testing.

The second observation here is that the efficacy of isolation of the positive cases plays a direct and important role in the success of a mass testing campaign. Consider $\mathcal{E}$ to be the ratio of infectiousness of isolated cases with respect to the symptomatic ones. It is straightforward to see that each detection rate is reduced by the factor $(1 - \mathcal{E})$, resulting in less efficient mass testing as shown in figure 5c.

Mitigation study

In this section we investigate the effect of two different mitigation strategies: social distancing and mass testing. It is important to point out that our results have to be seen relative to the base case without mitigation. As the estimated parameters all come with uncertainty, the numerical results are subject to quantitative errors, but they provide a qualitative picture of the essential dynamics.

The first mitigation strategy tested with our model was social distancing for 150 days (from day 50 till day 200); see figures 6b and 6c. Dashed lines represent the immune ($n_s^0 - n_s$), dash-dotted lines the infected ($n_i^{undet} + n_i^{det}$) and solid lines the deceased (n_d^{tot}) populations, on the upper panel with linear and in the middle panel with logarithmic scaling. The grey shading marks the "social distancing" phases. For comparison, figure 6a shows the base case. For the case in figure 6b, the infection rate was re-

Figure 4: Mass testing. The number of tests required to reach $\mathcal{R}_{\text{eff}} = 1$ depends on the time from sampling to result. A mitigation strategy relying on mass testing alone is assumed and we computed the number of tests performed per day, which are needed to achieve a particular test-speed dependent $\mathcal{R}_{\text{eff}}^{wt}/\mathcal{R}_0$ ratio; for (a) 5% and (b) 15% false negative test results are assumed. The green lines indicate $\mathcal{R}_{\text{eff}}^{wt} = 1$. Test speeds were: 0.5 days (black line), 1 day (orange line), 1.5 days (blue line) and 2 days (purple line).

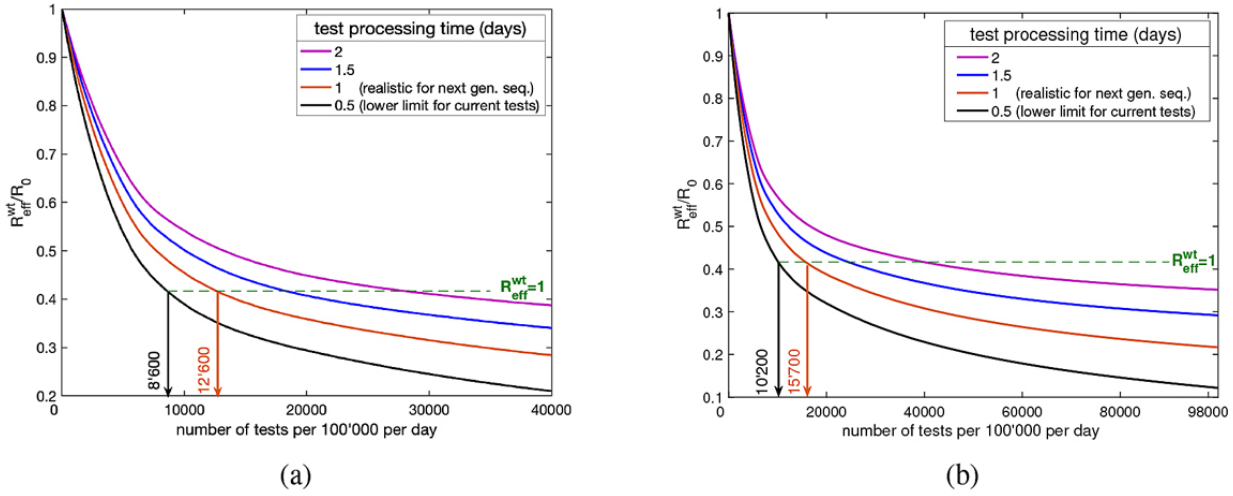

duced by 58%, corresponding to a virus reproduction number of $\mathcal{R}_{\text{eff}} = 1$. In the logarithmic plot the number of infected persons remains constant during the social distancing phase (as expected when $\mathcal{R}_{\text{eff}} = 1$ and $n_s \approx n_s^0$), but the number of cases and deaths keep increasing. Only a very small fraction of the endemic population is immune. With some delay after social distancing is abandoned, the numbers rise dramatically like in the base case, but about 150 days later.

Figure 6c shows the case with a 71% lower infection rate (corresponding to an effective reproduction number of 0.7). This time the reproduction number $\mathcal{R}_{\text{eff}}$ is smaller than 1 and therefore the number of infected persons declines exponentially, seen in the logarithmic plot. After the social distancing phase there is a delay of approximately 3 months before the numbers climb dramatically. In both cases the endemic state is almost the same as in the base case, i.e., temporary social distancing only delays the main outbreak. Thus, social distancing for a limited time alone is insufficient for resolving the basic problem. The success of a containment strategy eventually relies on discovering an effective and cheap vaccine in due time. Additional information regarding intensive care unit capacity is provided in the lower panel logarithmic plots of figure 6; shown are 20% of the strong symptomatic population (dotted lines) together with the intensive care unit capacity of 0.008% (horizontal long dashed lines).

The second mitigation strategy we investigated was mass testing with isolation of detected cases over the same period, that is, from day 50 till day 200. Figures 7b and 7c show the results obtained with an average testing interval of 7.92 days with 1 day processing time, which reduces

Figure 5: Sensitivity analysis of mass testing with 1 day delay time and a 5% false negative rate. A mitigation strategy relying on mass testing alone is assumed and we computed the number of tests performed per day, which are needed to achieve a particular $\mathcal{R}_{\text{eff}}^{\text{wt}}/\mathcal{R}_0$ ratio; for (a) fraction of asymptomatic cases: 50% (black line), 44% (orange line), 39% (blue line) and 33% (purple line); for (b) infectiousness of asymptomatic cases compared to symptomatic ones: 100% (black line), 70% (orange line), 40% (blue line) and 10% (purple line); for (c) infectiousness of isolated cases compared to symptomatic ones: 0% (black line), 10% (orange line), 20% (blue line) and 30% (purple line); for (d) recovery time of asymptomatic cases: 15 days (black line), 12 days (orange line), 10 days (blue line) and 8 days (purple line). The green lines indicate $\mathcal{R}_{\text{eff}}^{\text{wt}} = 1$.

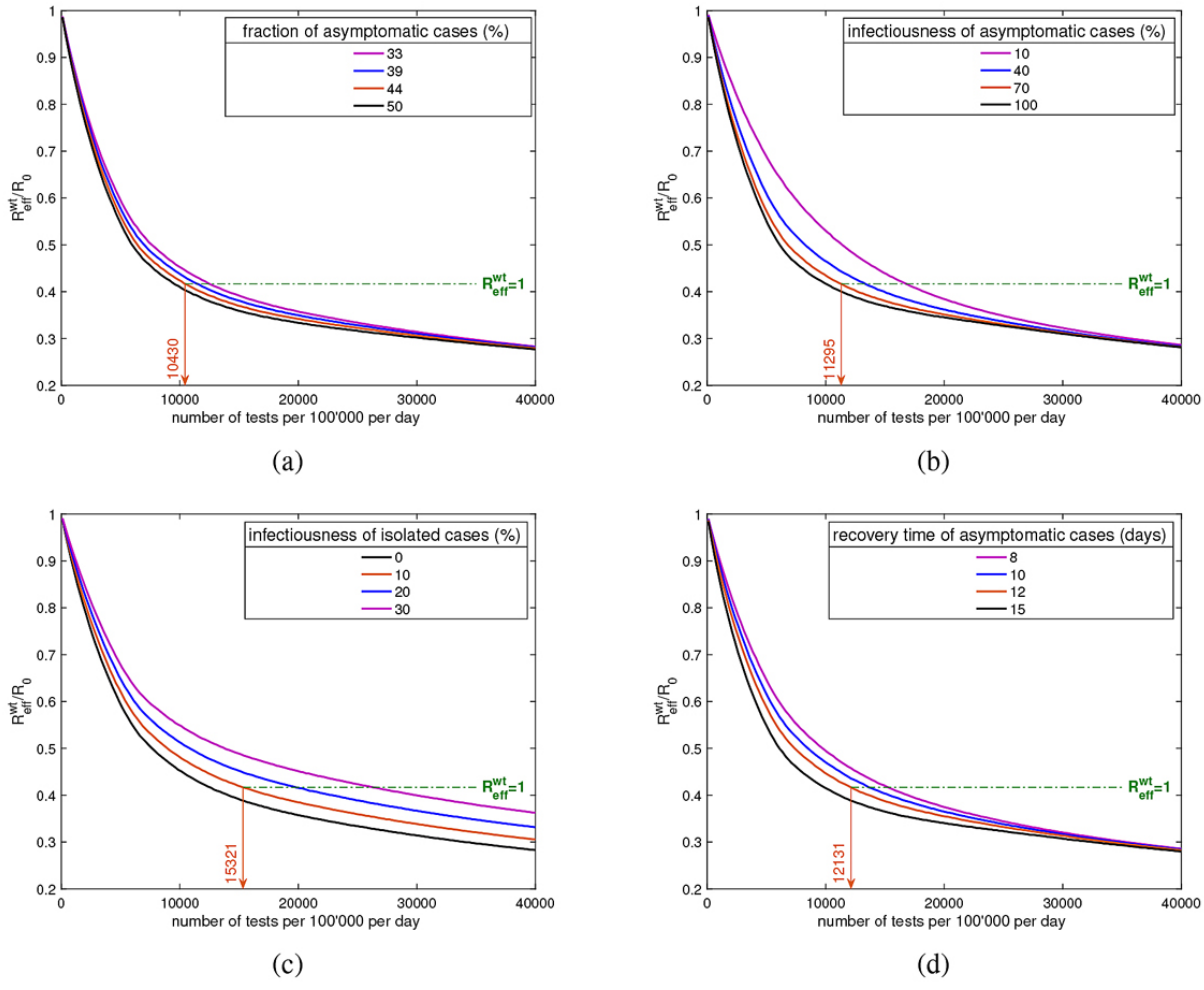

$\mathcal{R}_{\text{eff}}$ to 1 (with $k_e = 0.2097$, $k_s = 0.0242$ and $k_a = 0.0506$), and once with a testing interval of 2.68 days with 1 day processing time, which results in $\mathcal{R}_{\text{eff}} = 0.7$ (with $k_e = 0.5417$, $k_s = 0.0102$ and $k_a = 0.0052$). Dashed lines represent the immune ($n_s^0 - n_s$), dash-dotted lines the infected ($n_i^{undet} + n_i^{det}$) and solid lines the deceased (n_d^{tot}) populations, on the upper panel with linear and in the middle panel with logarithmic scaling. The gray shading marks the "mass testing" phases. These results are very similar as those shown in figure 6. For comparison the base case is shown in figure 7a.

This demonstrates that mass testing would have a similar effect as social distancing, and provided effective testing methods become available, this approach has the important advantage that the world's economy would not come to a halt. As in the case of social distancing, unless one assumes that the virus can be defeated completely and globally, testing would have to be continued until an effective vaccine becomes widely available. Again, information regarding

Figure 6: Social distancing from day 50 to day 200. (a) base case; (b) with a 58% lower infection rate (corresponding to a reproduction number of 1); (c) with a 71% lower infection rate (corresponding to a reproduction number of 0.7). Dashed lines represent the immune ($n_s^0 - n_s$), dash-dotted lines the infected ($n_i^{undet} + n_i^{det}$) and solid lines the deceased (n_d^{tot}) populations, on the upper panel with linear and in the middle panel with logarithmic scaling. The lower panel logarithmic plot shows 20% of the strongly symptomatic population (dotted lines) together with the intensive care unit capacity of 0.008% (horizontal long dashed lines). The values are in % of the initial susceptible population size and are plotted over number of days. The grey shading marks the "social distancing" phases.

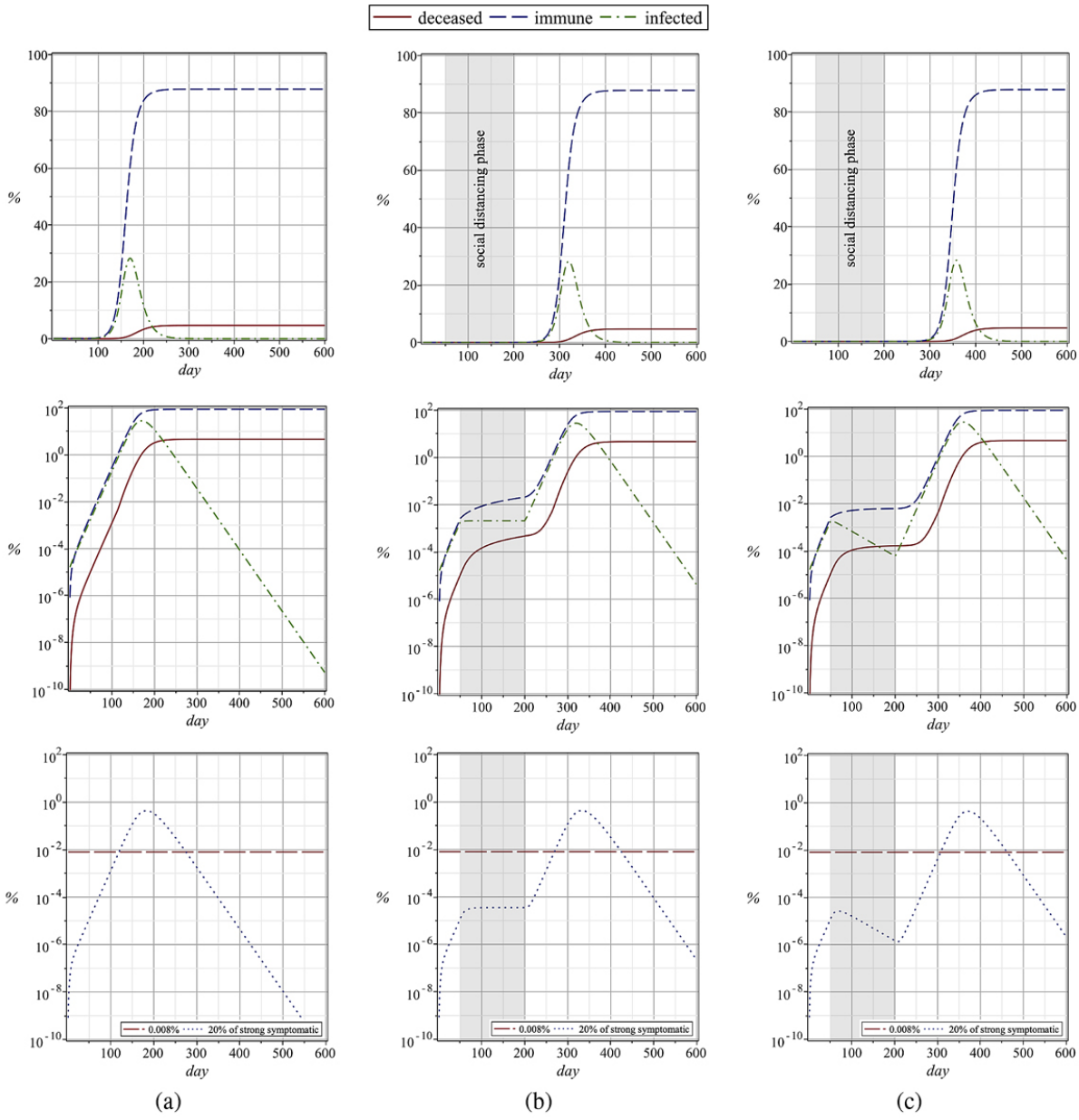

intensive care unit capacity is provided in the lower panel logarithmic plots of figure 7.

Finally, we investigated combination of social distancing and mass testing. Figure 8b shows a combination of social distancing followed by mass testing. From day 50 to 200, a 71% lower infection rate due to social distancing is considered, followed by a period of 100 days with a testing interval of 7.92 days with 1 day processing time.

Extreme social distancing brings the number of infections down and moderate mass testing keeps the values constant. Again, after the mass testing phase ends there is a delayed outbreak leading to almost the same endemic state as in the base case, which is shown in figure 8a. Figure 8c shows mass testing and social distancing at the same time from day 50 till day 300. It can be seen that reducing the infection rate by only 33%, a very long testing interval of 22.46 days and 1 day processing time is sufficient in this case to reduce the reproduction number to 1 and thus keep the size

Figure 7: Mass testing from day 50 to day 200. (a) base case; (b) with a testing interval of 7.92 days with 1 day processing time (corresponding to a reproduction number of 1); (c) with a testing interval of 2.68 days with 1 day processing time (reproduction number of 0.7). Dashed lines represent the immune ($n_s^0 - n_s$), dash-dotted lines the infected ($n_i^{undet} + n_i^{det}$) and solid lines the deceased (n_d^{tot}) populations, on the upper panel with linear and in the middle panel with logarithmic scaling. The lower panel logarithmic plot shows 20% of the strongly symptomatic population (dotted lines) together with the intensive care unit capacity of 0.008% (horizontal long dashed lines). The values are in % of the initial susceptible population size and are plotted over number of days. The grey shading marks the "mass testing" phases.

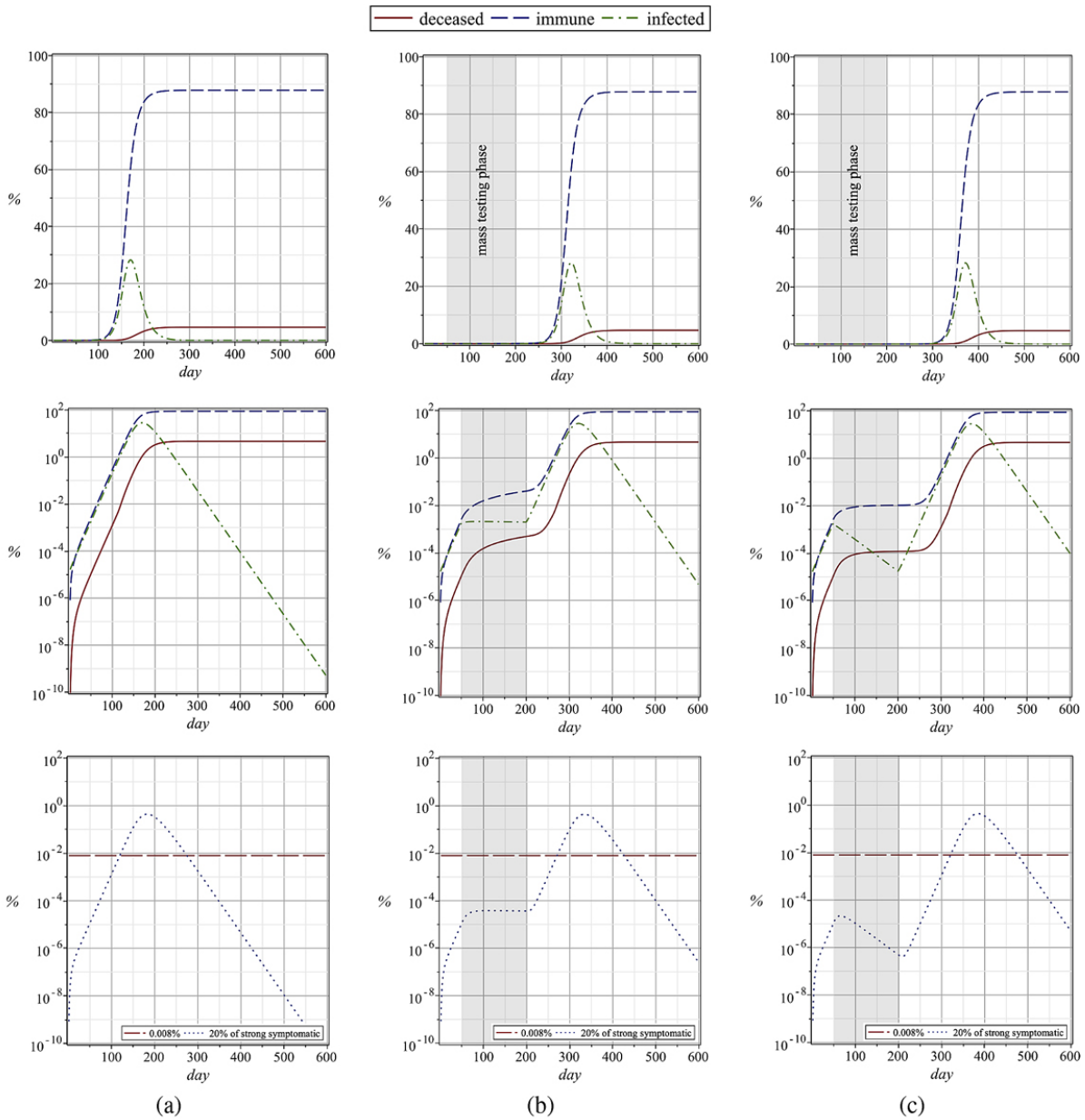

of the infected population constant. The lower panel logarithmic plots of figure 8 show 20% of the strongly symptomatic population (dotted lines) together with an intensive care unit capacity of 0.008% (horizontal long dashed lines). Overall, this shows that the "edge" gained by social distancing can be maintained by shifting mitigation towards moderate mass testing.

Contact tracing

Contact tracing has been proposed to slow down or even stabilise the pandemic [24, 35, 36]. The strategy is that symptomatic individuals who go into self-quarantine will use indirect contact information (including that from an app) to alert all proximity contacts of the past 2 weeks. In practice, either symptomatic individuals contact their close relatives and friends with whom they had contact, or other unknown contacts will be contacted by the authorities or by the app. It is clear that in order to make contact tracing work, prevalence and infectiousness must be low before symptoms arise. The latter turned out not to be the case for COVID-19, as infectiousness for up to 4–5 days before symptoms is possible [2], and a large fraction of cases remains asymptomatic with an infectious period of approximately 11–12 days [24].

Figure 8: Mass testing combined with social distancing. (a) base case; (b) social distancing phase from day 50 to day 200 with 71% lower infection rate followed by mass-testing period of 100 days with a testing interval of 7.92 days and one day processing time; (c) social distancing and mass testing at the same time from day 50 till day 300 with a 33% lower infection rate and a testing interval of 22.46 days and one day processing time.

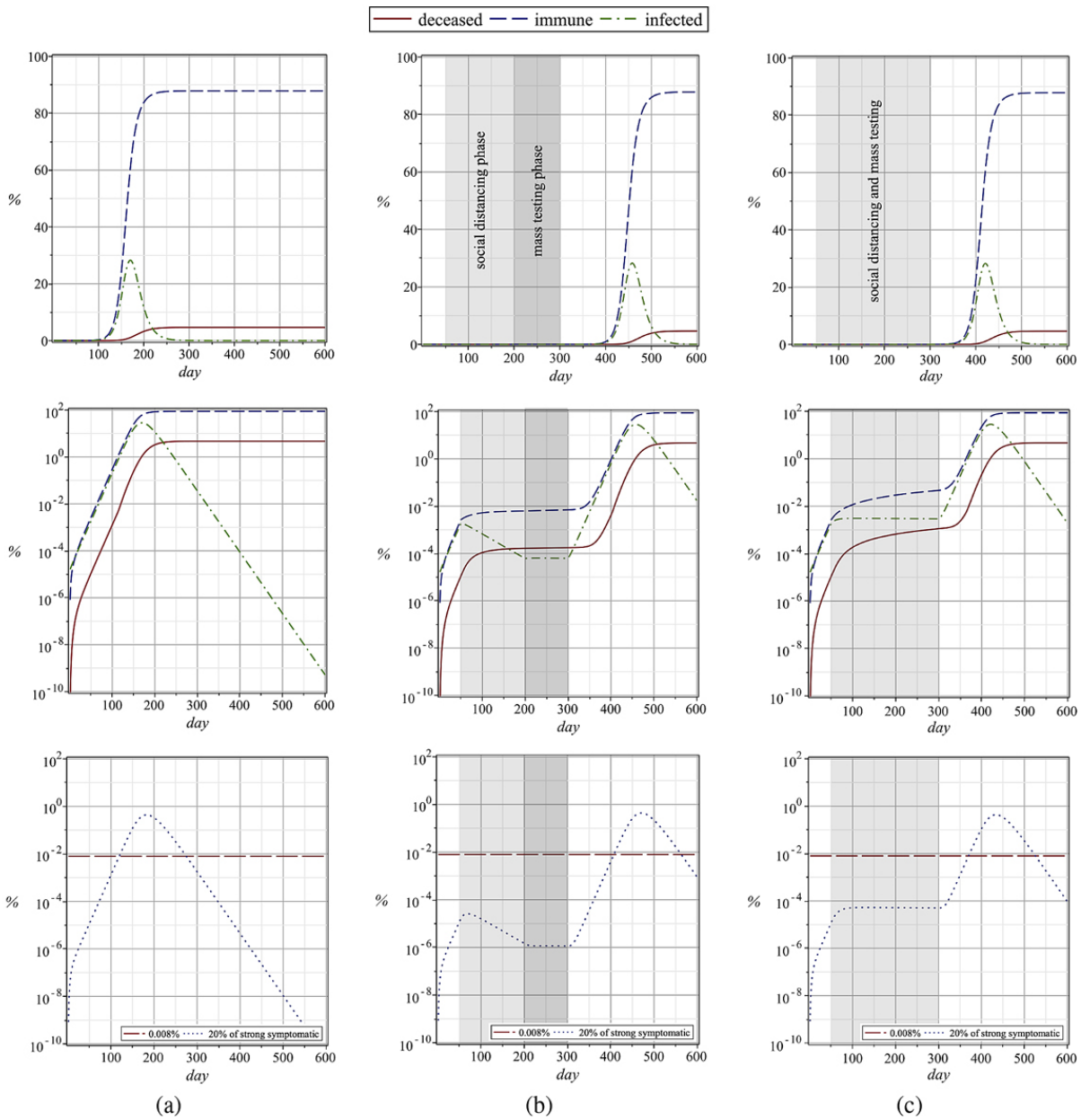

Here we present a simple analysis to find an upper bound on effectiveness of contact tracing. An idealised setting was considered, where we assumed that all symptomatic individuals participating in the scheme would perfectly self-isolate themselves after notifying the contact tracing system. Furthermore, we assumed that the notice-to-quarantine time is negligible [24, 35]. To parametrise the mitigation power of contact tracing, suppose r_1 is the fraction of asymptomatic individuals and r_2 is their infectiousness in comparison with symptomatic ones. The effective reproduction number resulting from contact tracing is derived below, for variables r_1 and r_2.

For both r_1 and r_2 different values are suggested in the literature. For r_1, one finds 1/3 in [19], 0.4 in [24] and 0.5 in [34], and for r_2 one finds 0.1 in [24], 2/3 in [19] and 1 in [37]. Based on these published numbers we considered $r_1 \in [0.3,0.5]$ and $r_2 \in [0.1,0.5]$. From equation (34) with our base case values $r_1 = 1/3$ and $r_2 = 0.5$, one obtains $\beta = 0.67$ (1/day), which is consistent with our previous parameter estimation. Based on our previous assumptions and on the values in table 2 we obtained $t_{ia} = \gamma_a^{-1} = 11.5$ days, $t_{im} = \xi_{ms}^{-1} = 1.5$ days and $t_{ms} = S^{(s)}\xi_{ss}^{-1} = 10$. Of interest here is the fraction

$$\kappa = \frac{\mathcal{R}_0^{sym}}{\mathcal{R}_0} = \frac{(1-r_1)(t_{im}+t_{ms}/10)}{r_1 r_2 t_{ia}+(1-r_1)(t_{im}+t_{ms}/10)} \quad (8)$$

of infected people who were infected by symptomatic cases, since this is the maximum relative reduction of $\mathcal{R}_0$ that can be achieved by tracing contacts of symptomatic individuals (by classical contact tracing or by using an app) with a success rate of $\zeta = 1$. Ignoring secondary infections (their probability becomes around 0.8%), we obtained the approximation

$$\mathcal{R}_{\text{eff}}^{ct} \approx [1-\zeta\kappa]\mathcal{R}_0 \quad (9)$$

for the effective reproduction number, if contact tracing is employed.

Figures 9a and 9b show the performance of contact tracing for different values of r_1, r_2 and ζ. The numbers attached to the isolines refer to the ratio $\mathcal{R}_{\text{eff}}^{wt}/\mathcal{R}_0$, and the bold contours depict combinations of r_2 and ζ for which $\mathcal{R}_{\text{eff}}$ is reduced from 2.4 to $\mathcal{R}_{\text{eff}}^{ct} = 1$. The effect of contact tracing, if applied only to identify contacts with symptomatic persons, is limited to optimistic assumptions concerning the parameters dictating the COVID-19 pandemic and strongly depends on size and infectiousness of the asymptomatic population relative to size and infectiousness of the symptomatic one. Even if the most optimistic assumptions would hold, more substantial reductions of $\mathcal{R}_{\text{eff}}$ would be desirable in order to accelerate the end of the pandemic (e.g., even in the absence of effective therapies or vaccines). For our base parameters of $r_1 = 1/3$ and $r_2 = 1/2$, contact tracing alone would not lead to an effective reproduction number of 1 (see fig. 9a at 50% infectiousness).

Discussion

As more and more affected populations are focusing on risk mitigation plans for COVID-19, it is important to identify strategies to mitigate and eventually suppress the pandemic. For this reason, it is crucial to understand the mechanisms underlying this pandemic-spread. Outcomes of social distancing and mass testing are investigated in this paper. It was found that the latter can significantly reduce the percentage of people getting infected and the death toll. It

Figure 9: Contact tracing: Effectiveness of contact tracing as a function of relative infectiousness of asymptomatic cases (r_2) and the success rate of contact tracing (ζ). (a) 33% of infected persons are asymptomatic ($r_1 = 0.33$); (b) 50% of infected persons are asymptomatic ($r_1 = 0.5$). The numbers attached to the isolines refer to the ratio $\mathcal{R}_{\text{eff}}^{wt}/\mathcal{R}_0$, and the bold contours depict combinations of r_2 and ζ for which $\mathcal{R}_{\text{eff}}$ is reduced from 2.4 to $\mathcal{R}_{\text{eff}}^{ct} = 1$. In all computations, notice-to-quarantine time was ignored and it was assumed that quarantined contacts are not infectious.

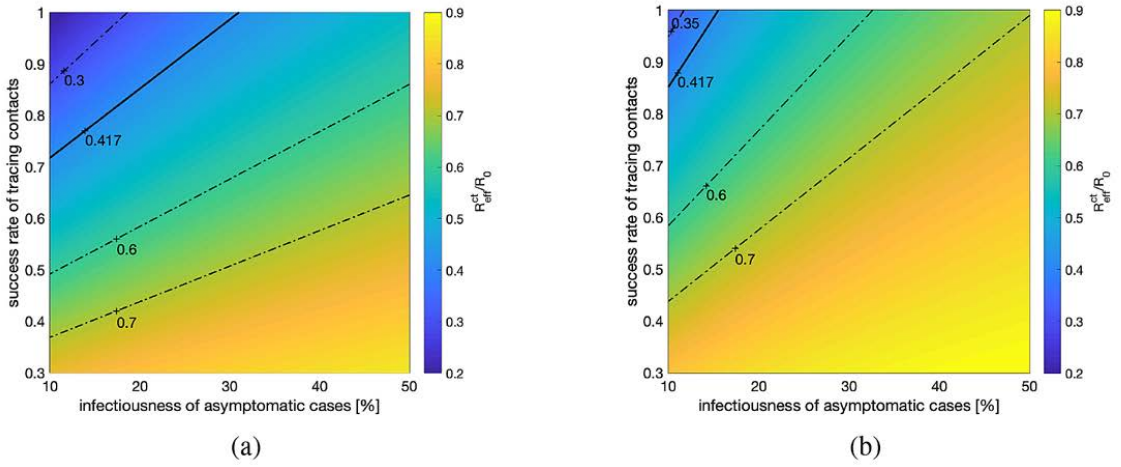

is important to emphasise here that repetitive testing of individuals without symptoms (if sufficiently large numbers of tests are available and can be applied) has a much stronger effect on the reproduction number than testing people with symptoms, since in most cases the latter are contained. As testing capacities improve, our approach may help to decide by how much social distancing measures can be relaxed. Whereas social distancing is currently essential, it is of utmost importance that testing capabilities are upgraded such that they cover large portions of affected populations in the near future.

From our analysis we conclude that testing every individual without symptoms every few days (with our assumptions roughly every week) would reduce the reproduction number of COVID-19 to 1 and thereby stabilise the pandemic, which is very promising. After a while, fewer and fewer infected people (who spread the virus) will be detected. In this way, continued large scale testing can verify the success of the mitigation strategy. Mass testing should be continued beyond this point, though at a reduced frequency. This would allow determination of whether the fraction of infected persons tends to increase. If this were the case, testing frequencies should again be ramped up. In any case, unless the virus can be defeated completely and globally by reducing the number of infected individuals to zero, there is a risk of COVID-19 re-emergence after such mitigation measures are abandoned.

In this context, the estimates for mass testing that are provided by our analysis should be regarded as estimates for the upper boundary of the tests needed. This upper boundary test number can be used as a guideline for development of mass testing technology and logistics. For further improvements of the predictions a more reliable data base for parameter tuning would be necessary. The model itself can be refined by accounting for different age groups and latency, which would involve additional parameters. In the future it would be of utmost interest to further investigate combined strategies such as social distancing for old and endangered persons and mass testing for the remaining population, including the work force. Ideally, contact tracing and repetitive testing should be combined with some sort of social distancing to successfully suppress the virus spread and to keep the death toll low.

Correspondence:
Dr Hossein Gorji
Empa Materials Science
and Technology
Ueberlandstrasse 129
CH-8600 Dübendorf
mohammadhossein.gorji[at]empa.ch

Acknowledgement
The authors are very thankful to Alexandre Duc for his contribution to the former version of the manuscript with a bluetooth app-based implementation of targeted testing, Dario Ackermann for the website corona-lab.ch, containing the simulation tool based on the model presented in this paper, and Emma Slack, Erik Bakkeren and Noemi Santamaria for helpful comments on the manuscript. Hossein Gorji acknowledges the funding provided by Swiss National Science Foundation under the grant number 174060.

Disclosure statement
No potential conflict of interest relevant to this article was reported.

References

1 Tracy M, Cerdá M, Keyes KM. Agent-Based Modeling in Public Health: Current Applications and Future Directions. Annu Rev Public Health. 2018;39(1):77–94. doi:https://doi.org/10.1146/annurev-publhealth-040617-014317. PubMed

2 Ball F, Sirl D, Trapman P. Analysis of a stochastic SIR epidemic on a random network incorporating household structure. Math Biosci. 2010;224(2):53–73. doi:https://doi.org/10.1016/j.mbs.2009.12.003. PubMed

3 Kiss IZ, Miller JC, Simon PL. Mathematics of epidemics on networks. Vol. 46. Springer; 2017.

4 Allen LJS, Bauch CT, Castillo-Chavez C, Earn DJD, Feng Z, Lewis MA, et al. Mathematical Epidemiology. Brauer F, van den Driessche P, Wu J, editors. 2008. 415 p.

5 Siettos CI, Russo L. Mathematical modeling of infectious disease dynamics. Virulence. 2013;4(4):295–306. doi:https://doi.org/10.4161/viru.24041. PubMed

6 Daley DJ, Gani J. Epidemic modeling: an introduction. Cambridge: Cambridge University Press; 1999. 15.

7 Britton T. Stochastic epidemic models: a survey. Math Biosci. 2010;225(1):24–35. doi:https://doi.org/10.1016/j.mbs.2010.01.006. PubMed

8 Allen LJS. A primer on stochastic epidemic models: Formulation, numerical simulation, and analysis. Infect Dis Model. 2017;2(2):128–42. doi:https://doi.org/10.1016/j.idm.2017.03.001. PubMed

9 Zhou Y, Yuan S, Zhao D. Threshold behavior of a stochastic SIS model with Lévy jumps. Appl Math Comput. 2016;275:255–67. doi:https://doi.org/10.1016/j.amc.2015.11.077

10 Wu JT, Leung K, Leung GM. Nowcasting and forecasting the potential domestic and international spread of the 2019-nCoV outbreak originating in Wuhan, China: a modelling study. Lancet. 2020;395(10225):689–97. doi:https://doi.org/10.1016/S0140-6736(20)30260-9. PubMed

11 Hou C, Chen J, Zhou Y, Hua L, Yuan J, He S, et al. The effectiveness of quarantine of Wuhan city against the Corona Virus Disease 2019 (COVID-19): A well-mixed SEIR model analysis. J Med Virol. 2020;92(7):841–8. doi:https://doi.org/10.1002/jmv.25827. PubMed

12 Rădulescu A, Williams C, Cavanagh K. Management strategies in a SEIR-type model of COVID 19 community spread. Sci Rep. 2020;10(1):21256. doi:https://doi.org/10.1038/s41598-020-77628-4. PubMed

13 He S, Peng Y, Sun K. SEIR modeling of the COVID-19 and its dynamics. Nonlinear Dyn. 2020;101(3):1667–80. doi:https://doi.org/10.1007/s11071-020-05743-y. PubMed

14 Block P, Hoffman M, Raabe IJ, Dowd JB, Rahal C, Kashyap R, et al. Social network-based distancing strategies to flatten the COVID-19 curve in a post-lockdown world. Nat Hum Behav. 2020;4(6):588–96. doi:https://doi.org/10.1038/s41562-020-0898-6. PubMed

15 Rockett RJ, Arnott A, Lam C, Sadsad R, Timms V, Gray K-A, et al. Revealing COVID-19 transmission in Australia by SARS-CoV-2 genome sequencing and agent-based modeling. Nat Med. 2020;26(9):1398–404. doi:https://doi.org/10.1038/s41591-020-1000-7. PubMed

16 Silva PCL, Batista PVC, Lima HS, Alves MA, Guimarães FG, Silva RCP. COVID-ABS: An agent-based model of COVID-19 epidemic to simulate health and economic effects of social distancing interventions. Chaos Solitons Fractals. 2020;139(10223):110088. doi:https://doi.org/10.1016/j.chaos.2020.110088. PubMed

17 BBC. Covid-19: China's Qingdao to test nine million in five days. 2020 Oct 12. Available from: https://www.bbc.com/news/world-asia-54504785

18 Li R, Pei S, Chen B, Song Y, Zhang T, Yang W, et al. Substantial undocumented infection facilitates the rapid dissemination of novel coronavirus (SARS-CoV-2). Science. 2020;368(6490):489–93. doi:https://doi.org/10.1126/science.abb3221. PubMed

19 Ferguson N, Laydon D, Nedjati Gilani G, Imai N, Ainslie K, Baguelin M, et al. Impact of non-pharmaceutical interventions (NPIs) to reduce COVID19 mortality and healthcare demand. 2020 Mar 16. Available from: http://spiral.imperial.ac.uk/handle/10044/1/77482

20 Diekmann O, Heesterbeek JA, Metz JA. On the definition and the computation of the basic reproduction ratio R0 in models for infectious diseases in heterogeneous populations. J Math Biol. 1990;28(4):365–82. doi:https://doi.org/10.1007/BF00178324. PubMed

21 Virlogeux V, Fang VJ, Wu JT, Ho L-M, Peiris JSM, Leung GM, et al. Brief Report: Incubation Period Duration and Severity of Clinical Disease Following Severe Acute Respiratory Syndrome Coronavirus Infection. Epidemiology. 2015;26(5):666–9. doi:https://doi.org/10.1097/EDE.0000000000000339. PubMed

22 Men K, Wang X, Yihao L, Zhang G, Hu J, Gao Y, et al. Estimate the incubation period of coronavirus 2019 (COVID-19). medRxiv. 2020;24(2):219.

23 Zhou F, Yu T, Du R, Fan G, Liu Y, Liu Z, et al. Clinical course and risk factors for mortality of adult inpatients with COVID-19 in Wuhan, China: a retrospective cohort study. Lancet. 2020;395(10229):1054–62. Available at: https://linkinghub.elsevier.com/retrieve/pii/S0140673620305663. doi:https://doi.org/10.1016/S0140-6736(20)30566-3. PubMed

24 Ferretti L, Wymant C, Kendall M, Zhao L, Nurtay A, Abeler-Dörner L, et al. Quantifying SARS-CoV-2 transmission suggests epidemic control with digital contact tracing. Science. 2020;368(6491):eabb6936–9. doi:https://doi.org/10.1126/science.abb6936. PubMed

25 Anastassopoulou C, Russo L, Tsakris A, Siettos C. Data-based analysis, modelling and forecasting of the COVID-19 outbreak. PLoS One. 2020;15(3):e0230405–21. doi:https://doi.org/10.1371/journal.pone.0230405. PubMed

26 Liu Y, Gayle AA, Wilder-Smith A, Rocklöv J. The reproductive number of COVID-19 is higher compared to SARS coronavirus. J Travel Med. 2020;27(2): taaa021. doi:https://doi.org/10.1093/jtm/taaa021. PubMed

27 Liu Z, Bing X, Zhi XZ; Epidemiology Working Group for NCIP Epidemic Response, Chinese Center for Disease Control and Prevention. [The epidemiological characteristics of an outbreak of 2019 novel coronavirus diseases (COVID-19) in China]. Zhonghua Liu Xing Bing Xue Za Zhi. 2020;41(2):145–51. Article in Chinese. doi:10.3760/cma.j.issn.0254-6450.2020.02.003. PubMed

28 Karagiannidis C, Mostert C, Hentschker C, Voshaar T, Malzahn J, Schillinger G, et al. Case characteristics, resource use, and outcomes of 10 021 patients with COVID-19 admitted to 920 German hospitals: an observational study. Lancet Respir Med. 2020;8(9):853–62. doi:https://doi.org/10.1016/S2213-2600(20)30316-7. PubMed

29 Baud D, Qi X, Nielsen-Saines K, Musso D, Pomar L, Favre G. Real estimates of mortality following COVID-19 infection. Lancet Infect Dis. 2020;20(7):773. doi:https://doi.org/10.1016/S1473-3099(20)30195-X. PubMed

30 Mizumoto K, Chowell G. Estimating Risk for Death from Coronavirus Disease, China, January-February 2020. Emerg Infect Dis. 2020;26(6):1251–6. doi:https://doi.org/10.3201/eid2606.200233. PubMed

31 McIntosh K, Hirsch MS, Bloom A. Coronavirus disease 2019 (COVID-19) [Internet]. UpToDate; 2020. Available from: https://www.cmim.org/PDF_covid/Coronavirus_disease2019_COVID-19_UpToDate2.pdf

32 Corman VM, Landt O, Kaiser M, Molenkamp R, Meijer A, Chu DK, et al. Detection of 2019 novel coronavirus (2019-nCoV) by real-time RT-PCR. Euro Surveill. 2020;25(3):1–8. doi:https://doi.org/10.2807/1560-7917.ES.2020.25.3.2000045. PubMed

33 Hossain A, Reis AC, Rahman S, Salis HM. A massively parallel COVID-19 diagnostic assay for simultaneous testing of 19200 patient samples. Google Docs. 2020. Available from: https://docs.google.com/document/d/1kP2w_uTMSep2UxTCOnUhh1TMCjWvHEY0sUUpkJHPYV4/edit

34 Verity R, Okell LC, Dorigatti I, Winskill P, Whittaker C, Imai N, et al. Estimates of the severity of coronavirus disease 2019: a model-based analysis. Lancet Infect Dis. 2020;20(6):669–77. doi:https://doi.org/10.1016/S1473-3099(20)30243-7. PubMed

35 Hinch R, Probert WJM, Nurtay A, Kendall M, Wymatt C, Hall M, et al. OpenABM-Covid19 - an agent-based model for non-pharmaceutical interventions against COVID-19 including contact tracing. medRxiv. 2021 Jan 30:1–23.

36 Fraser C, Riley S, Anderson RM, Ferguson NM. Factors that make an infectious disease outbreak controllable. Proc Natl Acad Sci USA. 2004;101(16):6146–51. doi:https://doi.org/10.1073/pnas.0307506101. PubMed

37 Lavezzo E, Franchin E, Ciavarella C, Cuomo-Dannenburg G, Barzon L, Del Vecchio C, et al. Suppression of COVID-19 outbreak in the municipality of Vo. Nature. 2020;584(7821):425–9. doi:https://doi.org/10.1038/s41586-020-2488-1. PubMed

Appendix: Supplementary material

System of ordinary differential equations

The SEIR compartmental model consistent with the flowchart given in figure 1 takes the form

$$\dot{n}_s = -\beta\left(\frac{n_{ia}}{2} + n_{im} + \epsilon n_{ms}\right)\frac{n_s}{n_s^0} - Q\frac{n_s}{n_s^0}, \tag{10}$$

$$\dot{n}_e = \beta(n_{ia}/2 + n_{im} + \epsilon n_{ms})\frac{n_s}{n_s^0} - (\alpha_a + \alpha_s)n_e + Q\frac{n_s}{n_s^0} - k_e n_e, \tag{11}$$

$$\dot{n}_{ia} = \alpha_a n_e - \gamma_a n_{ia} - k_a n_{ia}, \tag{12}$$

$$\dot{n}_{im} = \alpha_s n_e - \xi_{ms} n_{im} - k_s n_{im}, \tag{13}$$

$$\dot{n}_{ra} = \gamma_a n_{ia}, \tag{14}$$

$$\dot{n}_{ms} = \xi_{ms} n_{im} - (\gamma_{ms} + \xi_{ss})n_{ms}, \tag{15}$$

$$\dot{n}_{ss} = \xi_{ss} n_{ms} - (\gamma_{ss} + \theta)n_{ss}, \tag{16}$$

$$\dot{n}_{rs} = \gamma_{ss} n_{ss} + \gamma_{ms} n_{ms} \quad \text{and} \tag{17}$$

$$\dot{n}_d = \theta n_{ss}. \tag{18}$$

Note that $\epsilon \in [0,1]$ is the transmission reduction factor of the self-isolated individuals. It is assumed that those infected persons who were detected by testing or hospitalized infect much less due to strong isolation and other precautions. Therefore, their effect on the infection rate is neglected here. In order to parametrize the model, besides the rates β, α_a, α_s, γ_a, γ_{ms}, γ_{ss}, ξ_{ms}, ξ_{ss} and θ, also the relative rate Q of infections from outside, i.e., by travel or from the animal world, has to be determined. Further, the initial values of $n_s(t)$, $n_e(t)$, $n_{ia}(t)$, $n_{im}(t)$, $n_{ra}(t)$, $n_{ms}(t)$, $n_{ss}(t)$, $n_{rs}(t)$ and $n_d(t)$ have to be chosen. The variables $\tilde{n}_e(t)$, $\tilde{n}_{ia}(t)$, $\tilde{n}_{im}(t)$, $\tilde{n}_{ra}(t)$, $\tilde{n}_{ms}(t)$, $\tilde{n}_{ss}(t)$, $\tilde{n}_{rs}(t)$ and $\tilde{n}_d(t)$ denote the respective numbers of persons who were tested positive and thus are removed from transmission. The detection rates of exposed (n_e), asymptomatic (n_{ia}) and mild symptomatic (n_{im}) persons due to testing are proportional to k_e, k_a and k_s, respectively. These individuals are then accounted for by the respective numbers $\tilde{n}_e(t)$, $\tilde{n}_{ia}(t)$ and $\tilde{n}_{im}(t)$; see figure S1. Note

Figure S1: Graph showing the dependencies of the compartments describing the dynamics of the positively tested people.

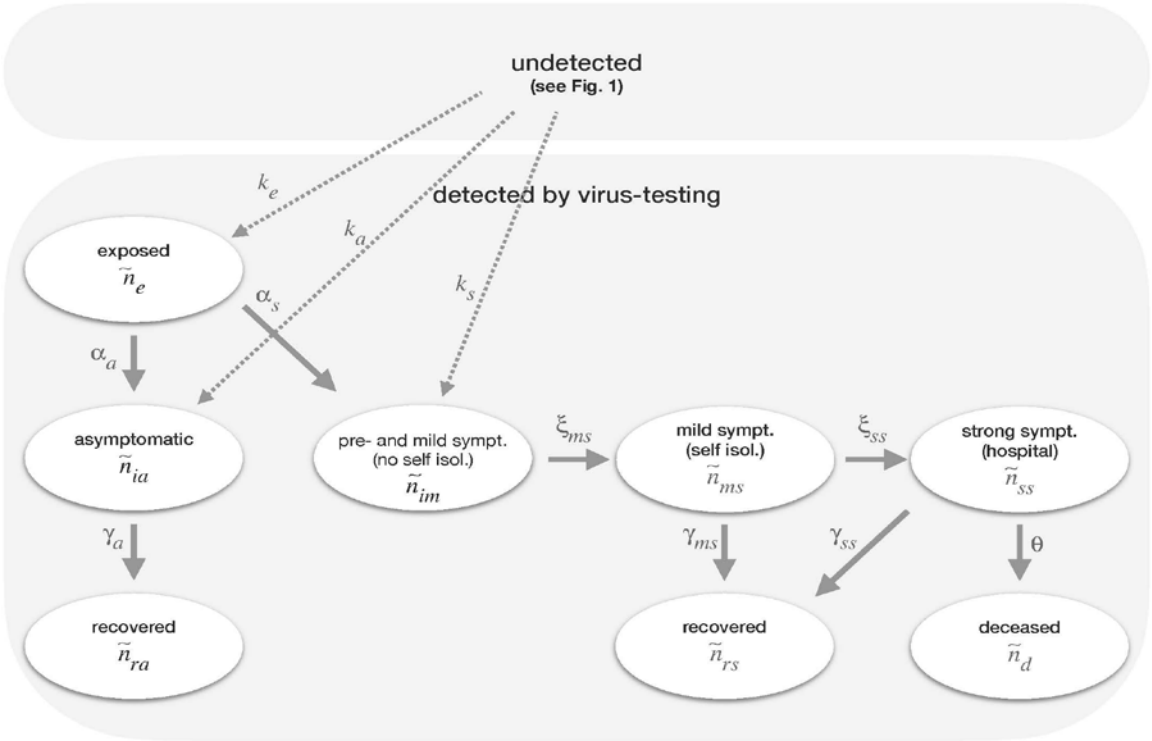

that the graph in figure S1 is very similar as the one in figure 1, except that there is no compartment for susceptible persons (since by definition a susceptible person cannot be detected infected) and that there exist sources due to testing (dotted arrows) instead of sinks.

To account for the dynamics with testing, the system in equations (10)-(18) has to be augmented by the ordinary differential equations

$$\dot{\tilde{n}}_e = -(\alpha_a + \alpha_s)\,\tilde{n}_e + k_e n_e, \tag{19}$$
$$\dot{\tilde{n}}_{ia} = \alpha_a\,\tilde{n}_e - \gamma_a\,\tilde{n}_{ia} + k_a n_{ia}, \tag{20}$$
$$\dot{\tilde{n}}_{im} = \alpha_s\,\tilde{n}_e - \xi_{ms}\,\tilde{n}_{im} + k_s n_{im}, \tag{21}$$
$$\dot{\tilde{n}}_{ra} = \gamma_a\,\tilde{n}_{ia}, \tag{22}$$
$$\dot{\tilde{n}}_{ms} = \xi_{ms}\,\tilde{n}_{im} - (\gamma_{ms} + \xi_{ss})\,\tilde{n}_{ms}, \tag{23}$$
$$\dot{\tilde{n}}_{ss} = \xi_{ss}\,\tilde{n}_{ms} - (\gamma_{ss} + \theta)\,\tilde{n}_{ss}, \tag{24}$$
$$\dot{\tilde{n}}_{rs} = \gamma_{ss}\,\tilde{n}_{ss} + \gamma_{ms}\,\tilde{n}_{ms} \quad \text{and} \tag{25}$$
$$\dot{\tilde{n}}_d = \theta\,\tilde{n}_{ss}. \tag{26}$$

Basic and effective reproduction numbers

To compute $\mathcal{R}_0$, we follow the next generation matrix method [1, 2] and split the dynamics of the infected population into the infection driven propagation f and the remainder V, i.e.,

$$\begin{bmatrix} \dot{n}_e \\ \dot{n}_{ia} \\ \dot{n}_{im} \\ \dot{n}_{ms} \\ \dot{n}_{ss} \end{bmatrix} = \overbrace{\begin{bmatrix} 0 & \beta/2 & \beta & \epsilon\beta & 0 \\ 0 & 0 & 0 & 0 & 0 \\ 0 & 0 & 0 & 0 & 0 \\ 0 & 0 & 0 & 0 & 0 \\ 0 & 0 & 0 & 0 & 0 \end{bmatrix}}^{f} \begin{bmatrix} n_e \\ n_{ia} \\ n_{im} \\ n_{ms} \\ n_{ss} \end{bmatrix} - \overbrace{\begin{bmatrix} \alpha_a + \alpha_s & 0 & 0 & 0 & 0 \\ -\alpha_a & \gamma_a & 0 & 0 & 0 \\ -\alpha_s & 0 & \xi_{ms} & 0 & 0 \\ 0 & 0 & -\xi_{ms} & \xi_{ss} + \gamma_{ms} & 0 \\ 0 & 0 & 0 & -\xi_{ss} & \theta + \gamma_{ss} \end{bmatrix}}^{V} \begin{bmatrix} n_e \\ n_{ia} \\ n_{im} \\ n_{ms} \\ n_{ss} \end{bmatrix}. \tag{27}$$

Note that testing is not considered here, i.e., k_e, k_a and k_s are zero. The $\mathcal{R}_0$ of this system is the spectral radius of fV^{-1}, that is,

$$\mathcal{R}_0 = \rho(fV^{-1}) = \frac{\beta\alpha_s}{\alpha_a + \alpha_s}\left[\frac{\alpha_a}{2\gamma_a\alpha_s} + \frac{1}{\xi_{ms}} + \frac{\epsilon}{\gamma_{ms} + \xi_{ss}}\right]. \tag{28}$$

To compute $\mathcal{R}_{\text{eff}}^{wt}$, the main dynamics of the infected population, which can be described by $[n_e(t), n_{ia}(t), n_{im}(t), n_{ms}(t), n_{ss}(t), \tilde{n}_e(t), \tilde{n}_{ia}(t), \tilde{n}_{im}(t), \tilde{n}_{ms}(t), \tilde{n}_{ss}(t)]^T$, is split into the rate of appearance f of new infected individuals and transfer $\tilde{V}$ of infected ones across different compartments, i.e.,

$$f = \begin{bmatrix} 0 & \beta/2 & \beta & \epsilon\beta & 0 & 0 & 0 & 0 & 0 & 0 \\ 0 & 0 & 0 & 0 & 0 & 0 & 0 & 0 & 0 & 0 \\ 0 & 0 & 0 & 0 & 0 & 0 & 0 & 0 & 0 & 0 \\ 0 & 0 & 0 & 0 & 0 & 0 & 0 & 0 & 0 & 0 \\ 0 & 0 & 0 & 0 & 0 & 0 & 0 & 0 & 0 & 0 \\ 0 & 0 & 0 & 0 & 0 & 0 & 0 & 0 & 0 & 0 \\ 0 & 0 & 0 & 0 & 0 & 0 & 0 & 0 & 0 & 0 \\ 0 & 0 & 0 & 0 & 0 & 0 & 0 & 0 & 0 & 0 \\ 0 & 0 & 0 & 0 & 0 & 0 & 0 & 0 & 0 & 0 \\ 0 & 0 & 0 & 0 & 0 & 0 & 0 & 0 & 0 & 0 \end{bmatrix} \tag{29}$$

and

$$\widetilde{V} = \begin{bmatrix} \alpha_a+\alpha_s+k_e & 0 & 0 & 0 & 0 & 0 & 0 & 0 & 0 & 0 \\ -\alpha_a & \gamma_a+k_a & 0 & 0 & 0 & 0 & 0 & 0 & 0 & 0 \\ -\alpha_s & 0 & \xi_{ms}+k_s & 0 & 0 & 0 & 0 & 0 & 0 & 0 \\ 0 & 0 & -\xi_{ms} & \xi_{ss}+\gamma_{ms} & 0 & 0 & 0 & 0 & 0 & 0 \\ 0 & 0 & 0 & -\xi_{ss} & \theta+\gamma_{ss} & 0 & 0 & 0 & 0 & 0 \\ -k_e & 0 & 0 & 0 & 0 & \alpha_a+\alpha_s & 0 & 0 & 0 & 0 \\ 0 & -k_a & 0 & 0 & 0 & -\alpha_a & \gamma_a & 0 & 0 & 0 \\ 0 & 0 & -k_s & 0 & 0 & -\alpha_s & 0 & \xi_{ms} & 0 & 0 \\ 0 & 0 & 0 & 0 & 0 & 0 & 0 & -\xi_{ms} & \xi_{ss}+\gamma_{ss} & 0 \\ 0 & 0 & 0 & 0 & 0 & 0 & 0 & 0 & -\xi_{ss} & \theta+\gamma_{ss} \end{bmatrix}, \quad (30)$$

which leads to

$$\mathcal{R}_{\text{eff}}^{wt} = \rho(f\,\widetilde{V}^{-1}) = \frac{\beta\alpha_s}{\alpha_a+\alpha_s+k_e}\left[\frac{\alpha_a}{2(\gamma_a+k_a)\alpha_s}+\frac{1}{\xi_{ms}+k_s}\left(1+\frac{\epsilon\xi_{ms}}{\gamma_{ms}+\xi_{ss}}\right)\right]. \quad (31)$$

Contact tracing

To analyze the effect of contact tracing on the effective reproduction number, the expected infectiousness $\widetilde{\beta}(\tau)$ at time τ after infection plays a central role. By knowing $\widetilde{\beta}(\tau)$ we can extract the basic reproduction number as

$$\mathcal{R}_0 = \int_0^\infty \widetilde{\beta}(\tau)d\tau. \quad (32)$$

Note that the above equation is consistent with our previous computation of $\mathcal{R}_0$ in the linear regime [3]. In our compartmental setting shown in Fig. 1 one obtains the expression

$$\widetilde{\beta}(\tau) = \sum_{i\in\mathcal{S}_c} \mathcal{P}_i\,\widetilde{\beta}_i(\tau), \quad (33)$$

where $\mathcal{P}_i$ is the probability that an infected individual is in compartment c_i, $\mathcal{S}_c = \{s, e, ia, ra, im, ms, rs, ss, d\}$ is the index set of all compartments and $\widetilde{\beta}_i(\tau)$ denotes the infectiousness at time τ after infection, if the individual is in c_i. Correspondingly, we denote the time spent in each compartment as $t_{i\in\mathcal{S}_c}$. From equations (32) and (33), if we assume that infectiousness is constant inside each compartment, we obtain

$$\mathcal{R}_0 = \overbrace{\beta r_1 r_2 t_{ia}}^{\mathcal{R}_0^{asym}} + \overbrace{\beta(1-r_1)\left(t_{im}+\frac{1}{10}t_{ms}\right)}^{\mathcal{R}_0^{sym}}, \quad (34)$$

where $r_1 = 1 - S^{(m)}$ is the fraction of exposed people who develop no symptoms (thus remain asymptomatic), and r_2 is the factor by which asymptomatic people are less infectious than symptomatic ones.

Model implementation

The dynamic model was implemented with Maple 2018. The calculations for mass testing and contact tracing were implemented with MATLAB and the Statistics Toolbox Release 2018b. The corresponding codes are available on GitHub server via https://github.com/gorjih2/STeCC_preliminary.

References

1 van den Driessche P, Watmough J. Reproduction numbers and sub-threshold endemic equilibria for compartmental models of disease transmission. Math Biosci. 2002;180(1-2):29–48. doi:https://doi.org/10.1016/S0025-5564(02)00108-6. PubMed

2 Zhao XQ. Dynamical systems in population biology. Springer; 2003.

3 Diekmann O, Heesterbeek JA, Metz JA. On the definition and the computation of the basic reproduction ratio R0 in models for infectious diseases in heterogeneous populations. J Math Biol. 1990;28(4):365–82. doi:https://doi.org/10.1007/BF00178324. PubMed